THERMAL DIFFUSIVITY OF PARTICULATE COMPOSITES MADE FROM ALUMINUM OXIDE AND NICKEL ALUMINIDE BY A PHOTOTHERMAL DEFLECTION TECHNIQUE

Y. D. CHUNG[1]†, A. P. CHOJNACKA[1], C. T. AVEDISIAN[1] and R. RAJ[2]‡

[1]Department of Mechanical and Aerospace Engineering, and [2]Department of Materials Science and Engineering, Cornell University, Ithaca, NY 14853, U.S.A.

Abstract—The photothermal deflection technique is used to measure the thermal diffusivity of a metal–ceramic composite. The present, as well as other data on composites are analyzed to estimate a value for the Kapitza radius, r_k, which represents the effective value of the thermal boundary resistance of heterointerfaces. Remarkably, the data from different metal–ceramic composite materials lead to a similar value (within a factor of about two), $r_k \approx 1\ \mu$m. Possible reasons for this outcome are discussed in terms of the acoustic mismatch model for thermal boundary resistance. Analysis of the data also suggests possible anomalous effects in nanostructured materials. © 1997 Acta Metallurgica Inc.

1. INTRODUCTION

The implementation of new materials into engineering systems requires the measurement and understanding of different kinds of properties. In high temperature structural applications, for example, not only mechanical but thermal properties need to be characterized and related to the microstructure. In materials with a metal–ceramic architecture, the large differences in the thermal expansion of the constituents, and low thermal conductivity of the ceramic phase, raise issues related to thermal stresses that are of special significance. The thermal boundary resistance of metal–ceramic interfaces can play a critical role in the overall behavior of the material, producing significant deviations from continuum models [1] that are built on the assumption that interfaces have negligible resistance to heat flow.

The thermal boundary resistance, R_{Bd}, was originally defined by Kapitza [2] in terms of a temperature drop, ΔT, that occurs across a planar interface between solid and liquid helium, in response to a heat flux, Q, in a direction normal to the interface:

$$R_{Bd} = \frac{\Delta T}{Q}. \qquad (1)$$

Equation (1) serves as a phenomenological description of the thermal boundary resistance of the interface. It does not concern the mechanisms and microstructure that control heat transport across the interface. It has been used to describe heat conduction across interfaces that are in atomic contact, as well as between two solids mechanically pressed together to create an interface where points of contact are discontinuous and microvoids control heat transfer across the interface (e.g. Ref. [3]). In the study of composites reported here we are mostly concerned with atomically bonded interfaces, although we should remain cognizant that plastic deformation and thermal stresses arising from a thermal expansion differential can cause local delamination at the interfaces within the composite.

In a composite material, where particles of one phase are dispersed in a matrix of another phase, R_{Bd} can cause the overall thermal conductivity of the composite to deviate from the continuum limit (from here onwards called the Maxwell limit [1]) when the contribution from interfaces becomes more important than the contribution from the volume of the

dispersed phase. The effect is stronger for smaller particles because they have a greater surface to volume ratio. The influence of R_{Bd} on composite behavior was first treated by Hasselman and Johnson [4] and later reduced to a different form by expressing R_{Bd} as a length scale, called Kapitza radius, r_k, which is related to R_{Bd} through the thermal conductivity of the matrix phase, K_m, as [5]

$$r_k = R_{Bd} K_m. \qquad (2)$$

The Kapitza radius is a useful engineering parameter because, generally speaking, it describes the transition where interfaces begin to have a significant influence on the thermal conductivity. When the particle radius is larger than r_k, the influence of interfaces may be ignored, but if the particle is smaller than r_k, then the thermal conductivity decreases as the particle size becomes smaller.

The thermal boundary resistance of metal–alumina interfaces has been measured [6] by depositing thin films of various metals on planar sapphire substrates and studying the heat transfer from the resistively heated film into the substrate underneath. This approach shows the systematic behavior of R_{Bd} at temperatures *below* the Debye temperature of the ceramic: following a T^{-3} dependence, as predicted by the acoustic mismatch theory. As the temperature approaches ≈ 50 K, however, there is a leveling off of the thermal boundary resistance. Interestingly this transition occurs at about the same temperature for many different kinds of metallic films on sapphire, and Swartz and Pohl [6] attribute this to scattering of high frequency phonons from the "rough" interfaces. There is little change in the thermal boundary resistance between approximately 50 K and room temperature for metal–alumina interfaces. The value for R_{Bd} near room temperature is estimated at 3 ± 10^{-8} m^2 K/W (to within a factor of two) from their measurements on interfaces between different metallic films and sapphire. Substituting $K_m = 27$–32 W/(mK) for sapphire into equation (2) yields $r_k = 0.80$–$0.96\ \mu$m, that is about $1\ \mu$m, for these interfaces.

Every et al. [5] employed an alternative method for estimating R_{Bd}, or in their case, r_k [see equation (2)]. By measuring the particle size dependence of the thermal conductivity of the composite, and then applying a modified version of the Hasselman and Johnson [4] analysis, a value of r_k could be obtained. The method was used to measure R_{Bd} for interfaces in a composite made from ZnS (matrix) and diamond (particles). A value of $1.5\ \mu$m for the Kapitza radius was deduced. Thus, in broad terms, the measurement of r_k for the composite agrees with measurements from the planar metal–ceramic interfaces studied by Swartz and Pohl [6].

In the present paper we present new measurements using the photothermal deflection (PD) spectroscopy technique (e.g. Refs [7, 8]) of the thermal diffusivity

of particulate composites consisting of an aluminum oxide matrix containing a dispersion of nickel aluminide (NiAl) particles, and made under controlled conditions in our own laboratory. The Kapitza radius for this system is estimated by measuring the change in the thermal diffusivity with particle size. Values are compared with several other metal–ceramic composites previously reported in the literature [9–11]. We show that a common value of r_k appears to exist, except for one measurement for composites made from nanosize particles which had an anomalously low thermal conductivity.

We begin by describing the experimental method for thermal diffusivity and show that it gives values accurate to better than 5% when compared against standard reference materials. Then we apply the technique to measure the thermal diffusivity of nickel-aluminide alumina composites. Since the materials were made by hot pressing we show the influence of microstructural anisotropy on the measurements. Finally we use measurements of thermal diffusivity to estimate r_k, and compare this estimate with values for r_k from other material systems.

2. MEASUREMENT OF THERMAL DIFFUSIVITY

The experimental method is illustrated in Fig. 1. A small spot on the specimen surface is heated by a laser (the "heating" beam). The heating beam is pulsed at a frequency "f" to create a steady periodic temperature field in the solid and air in contact with it. A second laser beam (the "probe" beam) is aligned nearly parallel to the surface of the specimen and bounces off it. The probe beam "bends" in the vicinity of the heated spot because the index of refraction of air is locally reduced. This bending serves as the signature of the thermal wave created by the heating beam. An analytical development for the probe beam deflection is then used to obtain thermal diffusivity by using the diffusivity as an adjustable parameter, rather like an inverse conduction problem. The frequency and energy of the heating beam, and the distance ξ (Fig. 1) are the control variables in the experiment.

While the full information available from measured probe beam deflection values can be used to obtain thermal diffusivity, Salazaar et al. [8] noted that for monolithic materials the first non-central zero, χ_0, of the variation of the in-phase or "real" part of the tangential component of the beam deflection with ξ varies linearly with $f^{-1/2}$ as

$$\chi_0 = c + \frac{m}{f^{1/2}} \qquad (3)$$

where c is a constant and the slope m is related to the thermal diffusivity, α, as:

$$m = b\sqrt{\pi\alpha}. \qquad (4)$$

Figure 2 shows a typical measurement of the variation of the real part of the tangential beam deflection (in arbitrary units) with the distance ξ (Fig. 1) for one of the standard reference materials which we used to calibrate our set-up (electrolytic iron) at a frequency of 2000 Hz. Figure 2(b) more clearly shows how χ_0 is determined from such measurements. A cross plot of χ_0 with $f^{-1/2}$ gives the result shown in Fig. 3. The linear variation is evident which is typical of the materials examined. These plots are further discussed later.

In equation (4), b is a constant determined by solving the coupled energy equations (e.g. Ref. [12]) for the air and solid, and then presenting the results in the form of equations (3) and (4) from which b is obtained. Three important assumptions in the analysis are that: (1) the dominant mechanism of heat transfer in the gas is conduction; (2) the incident laser power is absorbed at the surface (rather than distributed throughout the bulk); and (3) the material is isotropic. While the thermal diffusivities that match measured beam deflection values are dependent on the assumptions of the analysis, the raw beam deflection measurements are obviously not.

The first assumption limits the heating beam power to values that avoid natural convection in the air. On the other hand, to increase the signal to noise ratio the highest beam power is desirable. A balance is

determined by trial for given material systems. The extent to which the heating beam power is absorbed at the surface is determined by the absorption spectra for the test material and the wavelength of the heating beam. In the experimental set-up used here, the heating beam is an argon-ion laser (Coherent Innova 70-5 laser) capable of operating in either single-line or multiline wavelengths. The experiments were carried out using the dominant 514 nm wavelength line with the power kept to under 300 mW. At this wavelength, the NiAl–alumina composites are completely absorbing. The assumption of material isotropy is a restriction of the analysis (not for the measured beam deflection values, however). The extent of isotropy of the materials examined was assessed by scanning the heating beam across the surfaces of materials cut in two perpendicular directions. For the standard reference materials used to calibrate our instrumentation, no detectable difference in beam deflections were observed. The NiAl + alumina composites exhibited some anisotropy as discussed below due to the fabrication technique, but differences in average thermal diffusivity for the two directions were estimated to be typically less than 10%.

For a thermally thick solid (defined as one whose thickness is much greater than the thermal penetration depth), numerical analysis shows that $b \approx 1.2$. For a thermally thin solid in contact with a
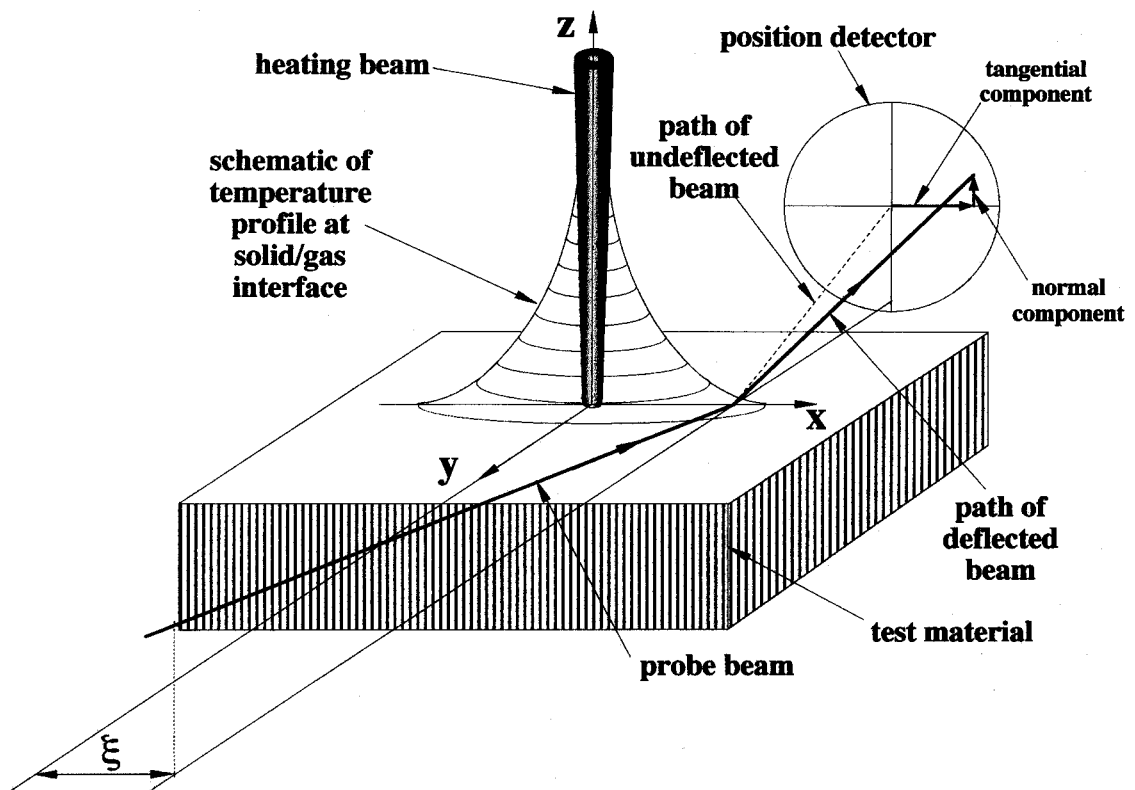

Fig. 1. A schematic of the experimental set-up for photothermal deflection spectroscopy. In the present approach only the tangential deflection is analyzed.
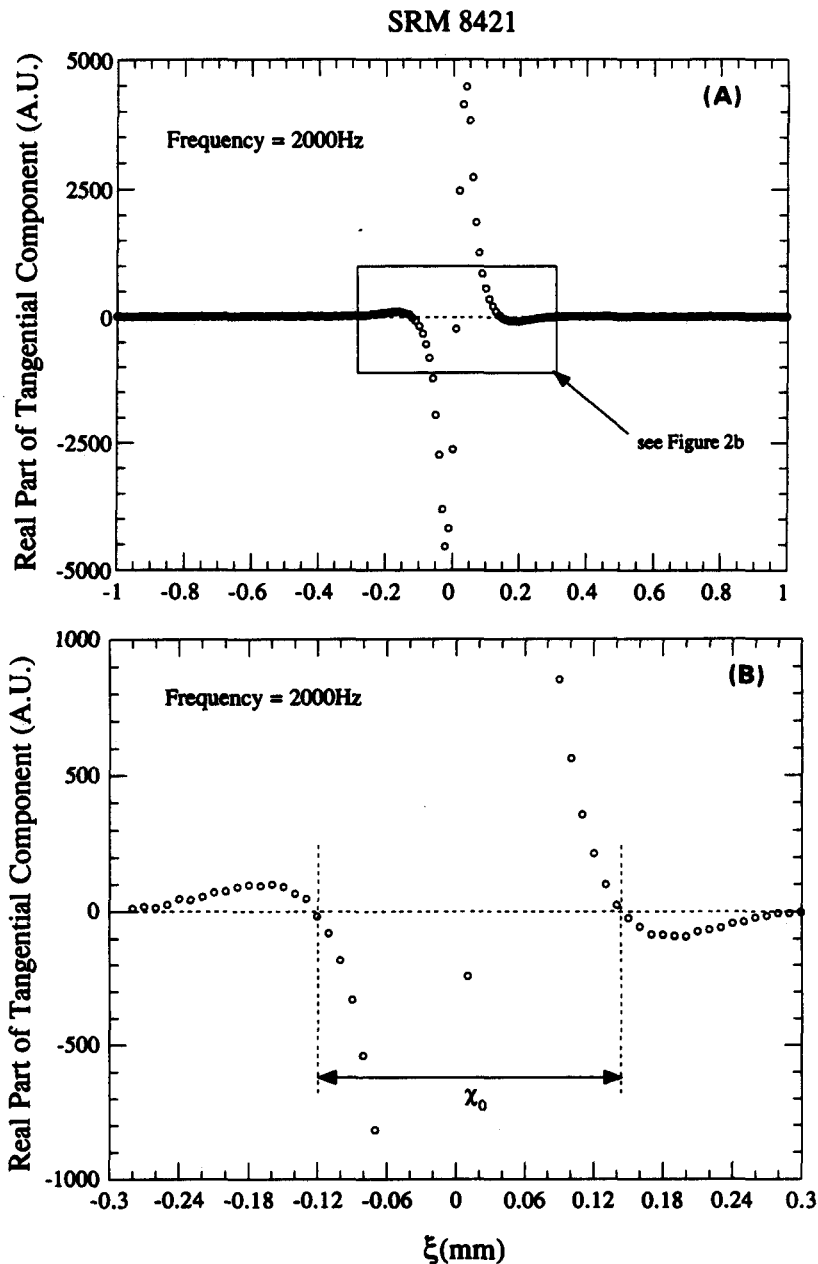
SRM 8421

Fig. 2. A plot of the real part of the tangential deflection plotted against the position of the incident beam in the x direction. The zero crossing is shown in the magnified plot.

media whose thermal conductivity is much less than the solid (e.g. air), $b \approx 1.0$ [12]. The materials examined here are thermally thick.

An experiment proceeds by first aligning the probe beam (a Uniphase U-130-P helium–neon laser) and heating beam by an automated process which involves stepping the heating beam in increments of 1–2 μm using computer controlled motion controllers in a given direction along the surface until the normal component of the probe beam deflection is maximum. Then, from this position the heating beam is scanned in a perpendicular direction until another

maxima is found. Similarly, the focal point of the heating beam is searched by moving the focal lens in the z direction (Fig. 1) until the normal component of the beam deflection is a maximum. The final aligned position is $x = y = z = 0$ in Fig. 1. In this computerized search process, the probe beam may either be "skimmed" along the test surface or "bounced" off it. Most of the data reported here were obtained by bouncing the beam because of the increased signal to noise ratio that results. Once aligned, the heating beam is systematically scanned across the sample while holding the modulation
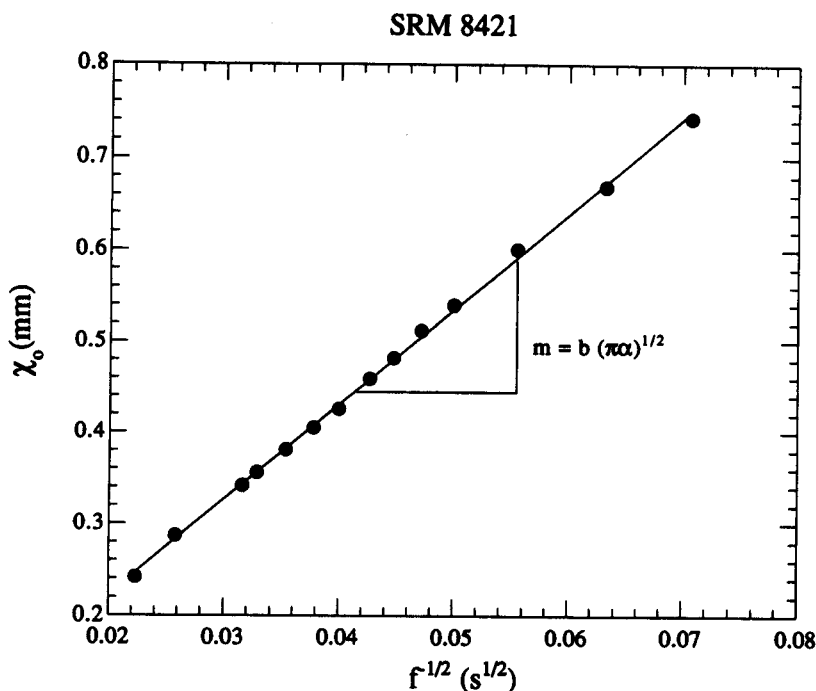
SRM 8421

Fig. 3. Variation of χ_0 with $f^{1/2}$ for a standard reference material, showing excellent fit to equation (3).

frequency constant. Typically, $-2\,\text{mm} < \xi < 2\,\text{mm}$ (e.g. Fig. 2) for the data analyzed. Outside this range, probe beam deflections are usually undetectable. At each position ξ, the tangential beam deflection components (real and imaginary parts) are stored by a lock-in amplifier (EG&G Princeton Applied Research model 5302) and subsequently transported to a PC-based data acquisition system. The lock-in reduces signal noise from the position sensor circuit (modulation frequencies equal to multiples of 60 Hz are avoided). Typical frequencies range from 10 to 10,000 Hz. Further details of the instrumentation and experimental procedures are given elsewhere [12].

Our experimental arrangement was calibrated using three standard reference materials (SRM) obtained from NIST: electrolytic iron (SRM-8421), stainless steel (SRM-1462), and graphite (SRM-8425). Figure 2 shows typical measurements of the real part of the tangential deflection at $f = 2000\,\text{Hz}$ for SRM-8421, and Fig. 3 illustrates the corresponding variation of χ_0 with $f^{-1/2}$; Fig. 4 shows a similar

plot for one of the NiAl–Al$_2$O$_3$ samples studied. The data show excellent fit to a straight line [equation (3)] for f ranging from 200 to 2000 Hz. Similar linearity was measured for the other two SRMs, and for the three alumina–NiAl composites we fabricated as noted below. The slopes from these linear fits combined with equation (3) yield the thermal diffusivity values of the SRMs listed in Table 1.

It is important to note that thermal diffusivity is dependent on temperature. The temperature to which the thermal diffusivity approximately corresponds was assessed by measuring the surface temperature at the focal point of the heating beam at the surface. A representative measure of this temperature was obtained by focusing the heating beam on to a type-E thin film thermocouple deposited on an alumina substrate. The maximum temperature rise was found to be 17 K for heating beam powers ranging from 2 to 295 mW and a modulation frequency of 1 Hz. Higher frequencies yielded lower temperatures. Over this temperature range, the NIST reported values varied by less than 2%. The NIST values listed in Table 1 are for room temperature. The agreement with our measured thermal diffusivities is within 5% of the NIST standard.

An interesting feature of the method is a direct measurement of the thermal penetration depth of the heating beam. As shown in Fig. 3, χ_0 ranges from 0.2 to 0.8 mm. Intuitively, χ_0 can be taken to be a measure of a radial width of the thermal wave established on a specimen, and so should be a useful length scale to which the microstructural and physical dimensions of the specimen can be compared to

Table 1. Thermal diffusivity of Standard Reference Materials

Standard material	Measured value (mm^2/s)	NIST value (mm^2/s)	% Error
Stainless steel (SRM-1462)	3.68	3.58	2.8
Electrolytic iron (SRM-8421)	24.0	22.9	4.8
Graphite (SRM-8425)	66.49	65.54	1.5

Table 2. Microstructural parameters for the NiAl (Al_2O_3) composites

	Powders		Metal dispersoids		
	p_{NiAl} (μm)	$p_{Al_2O_3}$ (μm)	v_f (%)	d (μm)	α (mm^2/s)
S1	10–20	0.2	33	10.2	6.8
S2	30–40	0.2	33	11.5	7.1
S3	40–50	0.2	33	23.3	7.9

determine their influence on the data. To be more accurate, the extent of the thermal wave is directly evidenced by measuring the beam deflection over the range of ζ.

3. PREPARATION AND CHARACTERIZATION OF COMPOSITES OF Al_2O_3 AND NiAl

Composites of NiAl + alumina were prepared by powder processing and hot pressing. The nickel aluminide powder was first sieved to obtain particles in the desired range (see Table 2). The NiAl particles were then mixed with 0.2 μm alumina powder in water using a spin bar and sonic dismembrator during which the mixture PH was regulated. The powder was dried, then ground in a ceramic vessel and vibration-milled for 3 h using alumina balls with a powder-to-ball weight ratio of 0.1. After milling, the mixture was ground again in a ceramic vessel and pressed into a graphite die. The composite was then placed into a furnace, evacuated to 50 mTorr and then the chamber was filled with argon. Constant flow of argon was maintained during the fabrication process. Densification of the alumina–NiAl mixture was accomplished in three stages: raising the temperature of the furnace to approximately 1400 K (at a rate of approximately 20 K/min), applying a constant uniaxial pressure of 30 MPa (at constant temperature for between 90 and 120 min), and release of the pressure and cooling down. Three types of specimens were prepared, all containing 67 vol% Al_2O_3, but using different initial particle sizes of the metallic phase.

The microstructural parameters of the three specimens, as well as the particle size of the starting powders, are listed in Table 2. In this table, p_{NiAl} and $p_{Al_2O_3}$ are the average particle sizes in the starting powders, v_f is the volume fraction of metal in the composite, and d is the particle size of the metal dispersoids in the ceramic matrix measured after hot pressing. The particle sizes were measured with the aid of a computer-based image analysis system. Because the particles are not spherical due to distortion caused by hot pressing, the numbers listed in Table 2 are average values. The values of thermal diffusivity, measured by the approach discussed in Section 2, as given in the right hand column, will be discussed later.

The microstructure of composites S1 and S3 are shown in Fig. 5. All micrographs were taken at the

same magnification to illustrate the difference in the particle size. Two cross sections, one taken perpendicular and the other parallel to the hot-pressing direction are shown. There is evidence of some anisotropy in the shape of the NiAl particles, as seen by some flattening of the particles in the direction running perpendicular to the hot-pressing axis. This is reflected in the small difference in the average thermal diffusivity in these two directions, due in part to the fact that the projected area between particles and matrix is larger in the plane perpendicular to hot pressing than parallel to it.

As noted previously, the data analysis assumes the material to be isotropoic so that m is related to α by equation (4). The change in particle shapes shown in Fig. 5 for two perpendicular directions raises the possibility that it is not for the NiAl–alumina composites. Average thermal diffusivities in the parallel and perpendicular planes to hot pressing differed by about 8% for composites of the type examined [12]. This difference reflects a combination of intrinsic error associated with estimating the thermal diffusivity (see Table 1), and that the analysis assumes an isotropic material, as noted above, while the materials examined in fact exhibit a difference in particle shape in perpendicular directions, as shown in Fig. 5. Since we were seeking a trend in the change in thermal diffusivity with particle size, we measured α for the same orientation of S1, S2 and S3 such that the specimen surface was aligned normal to the hot-pressing direction in the measurement of beam deflection. The resulting values of thermal diffusivity are given in Table 2.

Figure 4 shows a typical result for the variation of χ_0 with $f^{1/2}$ for the NiAl composites examined for heating beam scans in a plane normal to the direction of hot pressing. The example given is for the specimen S1. The linearity is evident (correlation coefficient was better than 0.99 for the three specimens). Using the values for m derived from results such as the one shown in Fig. 4, and assuming that $b \approx 1.2$, equation (4) was used to obtain the thermal diffusivity values shown in Table 2. Based on the intrinsic uncertainty in our method (Table 1) and variations in particle shape noted above, we expect our average measured values of the thermal diffusivity of the alumina–NiAl composites examined to deviate no more than between 10 and 15% from the absolute values for α (including possible anisotropy of thermal diffusivity).

4. ESTIMATES OF THE KAPITZA RADIUS

We use the expression for the thermal conductivity of the composite derived by Every et al. [5], which includes the influence of the thermal boundary resistance in the form of the Kapitza radius as defined in equation (2):

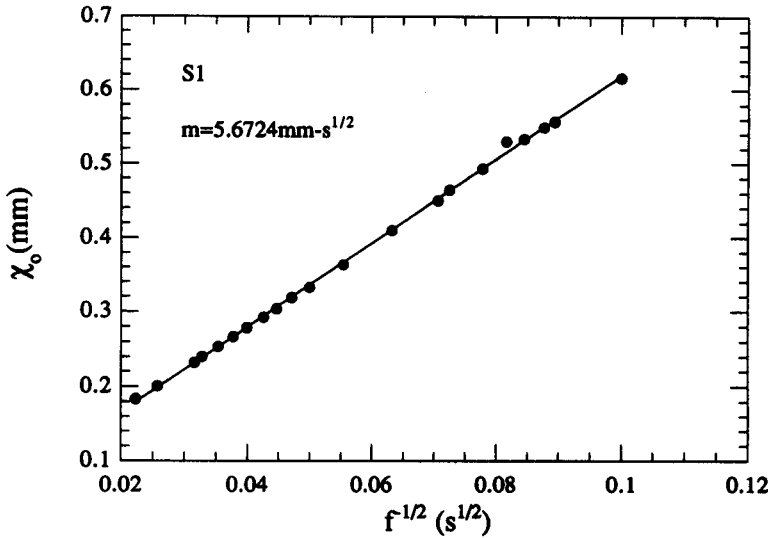$$\frac{K}{K_m} = 1 - 3v\frac{B - (1 - 2r_k/d)}{2B + (1 + 4r_k/d)}, \qquad (5)$$

Fig. 4. Variation of χ_0 with $f^{1/2}$ in the plane normal to the direction of hot pressing for the S1, Al$_2$O$_3$–NiAl composites examined (see Table 2). Value of m [equation (3)] is given in the inset. The line is a linear fit of the data. Correlation coefficient is better than 0.99 for the three composites.

where K is the thermal conductivity for the composite, and K_m for the matrix material by itself. B is the ratio of the thermal conductivities of the two constituents:

$$B = \frac{K_m}{K_d}, \qquad (6)$$

where K_d is the thermal conductivity of the dispersed phase. For the types of composites considered in this article, $B < 1$ as shown in Table 3.

As discussed earlier, the transient heat flow methods measure the thermal diffusivity. To compare with experiment it is easier if the result in equation (5) is normalized with respect to the continuum limit, derived by Maxwell [1], which corresponds to $R_{Bd} \to 0$, $r_k \to 0$, or $d \to \infty$. If the thermal conductivity of the composite in this limit is given by K_0, where K_0 is

$$\frac{K_0}{K_m} = 1 - 3v_f \frac{B-1}{2B+1}; \quad r_k \to 0 \qquad (7)$$

then it follows that

$$\frac{K}{K_m} = \frac{\alpha}{\alpha_0} \left[1 - 3v_f \frac{\dfrac{B-(1-2r_k/d)}{2B+(1+4r_k/d)} - \dfrac{B-1}{2B+1}}{1 - 3v_f \dfrac{B-1}{2B+1}} \right]. \qquad (8)$$

Note that the ratio of the thermal conductivities (K) has been equated to the ratio of the thermal diffusivities since the density (ρ) and the specific heat (C_p) of the composites should not be influenced by interfacial properties (recall that $K = \alpha \rho C_p$). The right-hand side in equation (8) approaches unity when $d \gg r_k$; physically this means that when the particles are much larger than the Kapitza radius, then the interfaces become inconsequential and the thermal diffusivity of the composite can be calculated from continuum models.

We now use the following approach for comparing data to equation (7), the purpose being to obtain an estimate of r_k. A value for α_0 is estimated by seeking an asymptotic trend for the data for very large particles sizes. With this value the parameter α/α_0 is plotted as a function of the particle size d and the fit to equation (8) is used to obtain an estimate for r_k.

The above approach is applied to four sets of data: (i) the Al$_2$O$_3$(NiAl) composites studied here; (ii) the Al$_2$O$_3$(Ni) composites studied by Liu *et al.* [9]; and (iii) the two sets of data from Al(SiC) composites studied by Geiger *et al.* [10] and Hasselman *et al.* [11]. The values for B, α_0 (or K_0) and v_f for each of these systems are given in Table 3. Here the constituent in brackets refers to the dispersed phase. Note that the

Table 3.

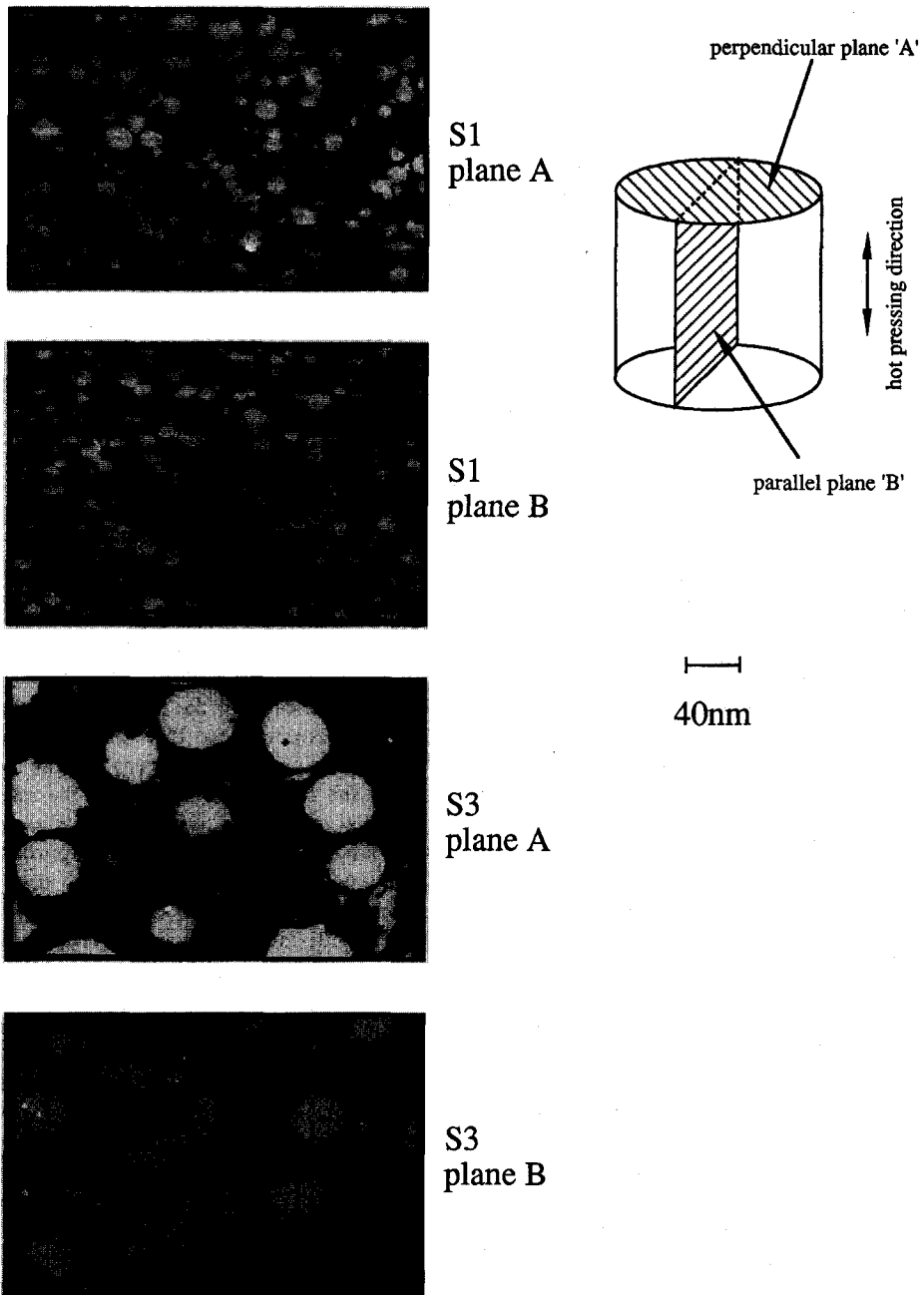| System	K_m (W/mK)	K_d (W/mK)	B (K_m/K_d)	v_f (%)	d (μm)	α_0 (mm^2/s)	K_0 (W/mK)	r_k (μm)
Al$_2$O$_3$ (NiAl)— this study	27.2	78	0.35	33%	10.2–23.3	8.2		1.5 $\pm$ 0.5
Al$_2$O$_3$ (Ni) [9]	32	59.3	0.135	5%	0.10–2.20		34	1.0 $\pm$ 0.5
Al (SiC) [10]	178	244	0.73	20%	0.70–28.0		215	$\approx$1.0
Al (SiC) [11]	178	244	0.73	40%	0.70–28.0		225	1.5 $\pm$ 0.5
ZnS (diamond) [5]	17.4	$\approx$600	0.03	10–30%	0.5–4.0	n/a	n/a	$\approx$1.0

Fig. 5. Scanning electron micrographs from S1 and S3 (see Table 2) for cross sections taken perpendicular and parallel to the hot-pressing directions. Note there is some degree of anisotropy in the microstructure.

data span not only different materials but also different particle sizes (0.1–28 μm) and volume fractions (5–40%).

The data are fitted to equation (8) in the following way. Plots of the α/α_0 vs d are constructed for the range of particle size, and for the values of v_f that are relevant to a particular composite. A family of curves for different r_k values are plotted on the same graph, and the measurements are placed on the graph. A visual comparison between the theoretical plots and

the data points gives an estimate of r_k which best describes the data.

The plots are given in Fig. 6 for the four composites described in Table 3. The fit is best for the aluminum–silicon carbide composite and a cautious agreement is obtained for the composites made from alumina–nickel aluminide. In the case of composites made with alumina and nickel [9] however, it is not possible to find agreement in any way with the model for the case where the particle size was 100 nm. For

the larger particle size the agreement with the model is reasonable.

If the 100 nm data point is excluded, then the four sets of data lead to estimates of r_k which are given in the right-hand column of Table 3, and fall in the range 0.5–2.0 μm.

5. DISCUSSION

As stated previously, the objective of this study is to present new measurements using the PD technique of the thermal diffusivity of particulate composites consisting of an aluminum oxide matrix and a dispersion of nickel aluminide (NiAl) particles, and to use the data to calculate the Kapitza radius, r_k, for these materials. The calculated value of r_k of the materials we fabricated, as well as for several other metal–ceramic composites reported in the literature [9–11], show a common value except for one measurement [9] for composites made from nanosize particles which had an anomalously low thermal conductivity.

The influence of interfacial resistance as measured by the Kapitza radius is considered to bridge the engineering significance of interfacial resistance in the design of material systems to the atomistic mechanisms of heat transfer across heterointerfaces. The Kapitza radius gives a length scale for the design of a laminated, fibrous, or particulate architecture of a bi-material. It marks the transition from interface dependent thermal diffusivity to interface independent thermal diffusivity of the composite. If the microstructural scale is smaller than r_k then interfaces have a large influence on α, but if it is greater then the interfacial effects are likely to be less important. The significance of this parameter to the design of composites, thin film architectures and multilayered thermal barrier coating is self evident.

The analysis of the data discussed in Section 4 leads to two findings:

(i) the value of the Kapitza radius is within a factor of 2, for several different material chemistries listed in Table 3, and,

(ii) the model for Kapitza radius that depends on assuming the material to have bulk properties on either side of the interface cannot be fit to the measurement of thermal conductivity in the alumina–nickel composite when the nickel particle size was only 100 nm.

The anomalous behavior of the composite discussed in (ii) above has been previously noted [9]. The thermal conductivity of the Al_2O_3–5 vol.% Ni composite, where $d_{Ni} = 100$ nm, was 26.4 W/(m/K). It has been noted [9] that assuming the particles to be insulating (equivalent to replacing them by holes,
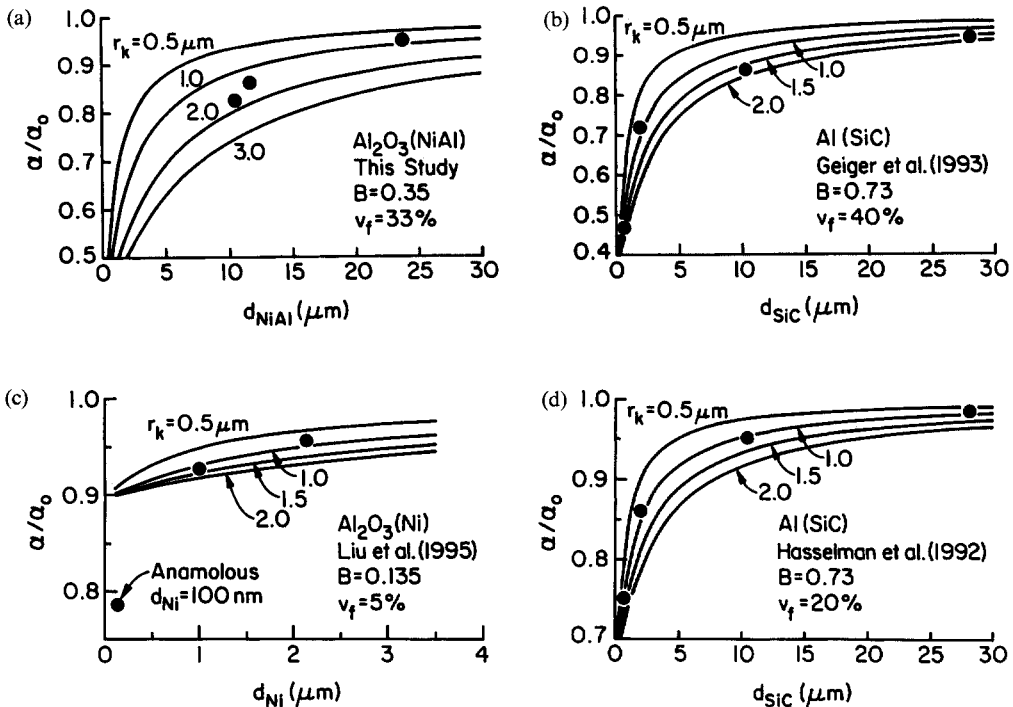

Fig. 6. Variation of composite thermal diffusivity with mean particle size. Solid lines are predictions from equation (8) and data points (●) are from the following sources: (a) present study; (b) Geiger et al. [10]; (c) Liu et al. [9]; (d) Hasselman et al. [11]. In each case v_f and B are held constant at values given in Table 3 and the Kapitza radius is varied over the range indicated. The anomaly (c) in the alumina–nickel composite for a particle size of 100 nm is noteworthy.

which would predict the lowest possible conductivity for the composite), leads to a theoretical lower limit of 29.6 W/(m/K) for the composite thermal conductivity. The experimental value lies below this limit. Liu *et al.* [9] mention a microstructural difference between the composites made with larger Ni particles [which are in agreement with equation (8)], and the $d_{Ni} = 100$ nm composite: the larger particles were placed at the grain boundaries of the alumina polycrystal but some Ni particles in the composite with the anomalous behavior were entrapped within the crystals of alumina. The higher and unrelaxed strain field in the nanocomposite noted previously [9] may, in fact, be the source of the discrepancy. (In very small particles the relaxation of thermal expansion strains by plastic deformation becomes less likely because of a lower probability of finding dislocations in them [13, 14].) Still, even if the elastic strains are large in the small particles, we do not have a mechanism that links the strains to thermal conduction. This may suggest that thermal boundary resistance of interfaces assumes a different character in nanostructured materials, and presumably is controlled by a different mechanism. Although we have only one measurement that suggests this possibility, when taken in perspective with the other data, it urges us to investigate the effect in greater depth and with different kinds of materials.

Turning to the point noted above that the Kapitza radius appears to have a common value for several different materials, the thermal resistance of an intercrystalline boundary can be visualized in terms of long wavelength phonons (at very low temperature) and short wavelength phonons (at higher T). The transition occurs at the Debye temperature. At low T, where the wavelengths are long, R_{Bd} can be analyzed in terms of an acoustic mismatch model which leads to a T^{-3} temperature dependence. As the Debye temperature is approached the phonon wavelength becomes comparable to the scale of atomic disorder at the interface, and R_{Bd} is expected to, and does [6], approach a value that is temperature independent. Thus, the thermal boundary resistance above the Debye temperature can be assumed to be equal to the thermal boundary resistance calculated from the acoustic mismatch model near the Debye temperature. Below we explore this concept further to explain why the Kapitza radius may be material independent.

In Ref. [5] it was pointed out that according to the acoustic mismatch model the Kapitza radius may be approximated in the following way:

$$100r_k = \frac{\lambda_{ph}}{\eta} \qquad (9)$$

where λ_{ph} is the mean free path of phonons, and η is the average probability for the transmission of the phonons into the ceramic phase. From the previous discussion, r_k at room temperature will be obtained by substituting a value for λ_{ph} that corresponds to the value that would be obtained near the Debye temperature of the material. Now, since λ_{ph} is likely to be similar for different materials near the Debye temperature (in view of the physical interpretation of the Debye temperature), it follows that r_k would also be similar for different materials, as long as η does not change significantly from one interface to another. The experiments and analysis reported here confirm this interpretation.

As a final point, we note that laser heating techniques typically rely on establishing a transient thermal wave in a material and then measuring the response of a signature variable to this wave (e.g. the probe beam deflection for the PD technique discussed here). The desired property is then obtained by matching the measured response variable with predictions of it from an analysis of heat transfer in the material. When laser heating creates a transient temperature field in the material, the thermal diffusivity, rather than the thermal conductivity, is measured. Fortunately, the thermal diffusivity itself is often the critical engineering parameter since the highest thermal stresses in components are generated during transient temperature loadings. Thus direct measurement of α can often be used in the analysis of thermal stresses in engineering components.

6. SUMMARY

The photothermal deflection technique is applied to measure the thermal diffusivity, α, of a metal–ceramic composite. The technique is capable of yielding absolute values of α with an accuracy of better than 5% for bulk materials. Anisotropic microstructure of the composite can lead to significant differences in the measurements made on surfaces cut in two orthogonal directions from an orthotropic material. The mean values of α in the plane perpendicular to hot pressing for the materials fabricated shows a trend towards lower diffusivity as the particle size of the dispersed phase is reduced, while keeping the volume fraction at a constant value. These data are consistent with measurements from other composite materials in the literature. All these data are analyzed in terms of a model where the thermal boundary resistance is expressed as a length scale, called the Kapitza radius, r_k. Interestingly, for the metal–ceramic composites analyzed all sets of data lead to a similar value for r_k, which is about 1 μm. This result is explained in terms of an acoustic mismatch model and the equivalence of the mean free path of the phonons in different materials near their respective Debye temperatures.

The Kapitza radius can serve as an engineering property of the interface that can be used to design the architecture and the microstructural scale of multiphase materials. If the microstructural scale is smaller than the Kapitza radius then the thermal behavior will depend primarily on the thermal

boundary resistance of the interfaces. If the microstructural scale is larger than r_k then the interface effects will be much less important.

REFERENCES

1. Maxwell, J. C., *A Treatise on Electricity and Magnetism*, Vol. 1, 3rd edn. Oxford University Press, Oxford, 1904.
2. Kapitza, P. L., *Collected Papers of P. L. Kapitza*, ed. D. ter Haar, Vol. 2. Pergamon Press, Oxford, 1965, p. 581.
3. Cooper, M. G., Mikic, B. B. and Yovanovich, M. M., *Int. J. Heat Mass Transf.*, 1969, **12**, 279.
4. Hasselman, D. P. H. and Johnson, L. F., *J. Comp. Mater.*, 1987, **21**, 508; see also Hasselman, D. P. H. in *Thermal Conductivity 20*, ed. D. P. H. Hasselman and J. F. Thomas Jr. Plenum Press, New York, 1989, p. 405.
5. Every, A. G., Tzou, Y., Hasselman, D. P. H. and Raj, R., *Acta metall. mater.*, 1992, **40**(1), 123.
6. Swartz, E. T. and Pohl, R. O., *Rev. Mod. Phys.*, 1989, **61**, 605.
7. Kuo, P., Inglehart, L., Sendler, E., Lin, M., Favro, L. and Thomas, R., *Review of Prog. in Quantitative Nondestructive Eval.*, 1985, **4B**, 745.
8. Salazaar, A., Sanchez-Lavega, A. and Fernandez, J., *J. Appl. Phys.*, 1989, **65**, 4150.
9. Liu, D. M., Tuan, W. H. and Chiu, C.-C., *Mater. Sci. Eng.*, 1995, **B31**, 287.
10. Geiger, A. L., Hasselman, D. P. H. and Donaldson, K. Y., *J. Mater. Sci. Lett.*, 1993, **12**, 420.
11. Hasselman, D. P. H., Donaldson, K. Y. and Geiger, A. L., *J. Amer. Ceram. Soc.*, 1992, **75**(11), 3137.
12. Chung, Y. D., *Thermal Property Measurements*, M.S. Thesis, Cornell University, Ithaca, NY, 1995.
13. Brenner, S. S., *J. Appl. Phys.*, 1956, **27**, 1484.
14. Thompson, L. R., *Acta metall. mater.*, 1994, **42**(7), 2477.